

| | | | |
|---|--|------------|---|
|  | SAKARYA UNIVERSITY JOURNAL OF SCIENCE | |  |
| | e-ISSN: 2147-835X http://www.saujs.sakarya.edu.tr | | |
| | Recieved | Accepted | |
| | 2017-04-05 | 2017-09-18 | 10.16984/saufenbilder.304203 |

Investigating the wear behaviour of induction hardened 100Cr6 steel

Gülcan Toktaş^{*1}, Alaaddin Toktaş², Murat Can Duran³

ABSTRACT

100Cr6 steel surface was induction hardened in order to be used in a bushing manufacturing. After examining the microstructure and hardness variations of the hardened surfaces, ball-on disc type wear tests were carried out. Wear tests were performed at 4,92 mm/s sliding speed, under various loads (2,5-5-10 N), in dry medium and at room temperature. The results of wear tests were evaluated by the mass loss method. The coefficients of friction were obtained during wear tests. The wear tracks and worn surfaces were investigated by optic and scanning electron microscopes. As a result, the surface hardness of the steel was obtained 2,5 times more than the core hardness by the aid of formed martensitic matrix structure instead of pearlitic one on steel surface by induction hardening process. It is seen that the highest mass loss was obtained by applying 5 N load in wear tests.

Keywords: 100Cr6 Steel, induction hardening, wear, mass loss

1. INTRODUCTION

Surface hardening processes come to manufacturer's rescue when machine parts need to be hardened only on the surface for a certain depth. Thus, the inner part remains soft and resistant for especially impact loads. In general, methods of surface hardening can be classified as thermochemical and thermal. In thermochemical process, machine part locates in high temperature medium with different chemical compositions for a while to let the atoms such as C, B and N to diffuse and make hard compounds on surfaces. Thermal case hardening differs from the former in the way of application. No chemical change occur on surface of a part in this method. Flame and induction hardening processes are two of the best known methods.

In induction hardening, heating is accomplished by placing a steel ferrous part in the magnetic field generated by high-frequency alternating current passing through an inductor, usually a water-cooled copper coil. The depth of heating produced by induction is related to the frequency of the alternating current, power input, time, part coupling and quench delay. The deeper case depths and even through hardening are produced by using lower frequencies. Some of the benefits of induction hardening are fast heating rates, energy efficiency, less distortion, cost savings, and small footprints [1, 2]. The fast heating rates result in structure refinement and better mechanical properties [2].

The other advantages of induction hardening can be listed as follows [3]:

- With a short heating time, there is no danger austenite grains would grow, which also means

¹ Balıkesir University, Faculty of Engineering, Mechanical Engineering Department, Çağış Campus, Balıkesir - gzeytin@balikesir.edu.tr

² Balıkesir University, Faculty of Engineering, Mechanical Engineering Department, Çağış Campus, Balıkesir - atoktas@balikesir.edu.tr

³ Balıkesir Metropolitan Municipality, Department of City Aesthetics, Balıkesir - mcanduran@yahoo.com

that there is no danger of formation of coarse and brittle martensite.

- The quenching procedure is easy to perform, contributing to short surface hardening times.
- A short procedure that does not require any additional protection against oxidation.
- Can be fully automated and is especially suitable for large series of workpieces.
- Induction hardening always leaves compressive residual stresses in the surface layer, which make machine components more resistant to dynamic loads.

100Cr6 (AISI 52100) steel, known as a member of bearing steels, is a high carbon and Cr alloyed steel which achieves a high degree of hardness with compressive strength and abrasion resistance used in ball and roller bearings, spinning tools, punches, and dies [4]. The surface hardness can be enhanced by induction hardening process. Machine tools, hand tools, crankshafts, camshafts, axle shafts, transmission shafts, universal joints, gears, pins, bearings are some examples of induction hardened machine parts [5].

Due to many advantages and wide application areas, studies and researches about induction hardening process are still going on. J. Yi et al. [6] reported that both induction hardening parameters (heating time and input power) and the initial hardness affect the distortion and hardening depth of samples. Lemos et al. [7] investigated the effect of bending+straightening process after induction hardened automotive drive shafts made of DIN 38B3. They emphasized that additional step of straightening changed the surface residual stress, caused higher microhardness values and deeper effective case depth. Sharma et al. [8] investigated the cracks encountered on crankshafts after induction hardening in terms of metallurgy. They reported some significant corrections and recommendations. Kusmoko et al. [9] studied the effects of induction temperatures range between 800-1200°C and tempering temperatures after induction hardening range between 300-700°C to the surface hardness and surface depth of SAE-AISI grade 1045 steel.

The goal of this study is to make a contribution in defense industry by revealing the tribological properties of induction hardened 100Cr6 steel. For this purpose, 100Cr6 steel surface was hardened by the optimal induction hardening process parameters and then, the effect of normal load on

tribological properties of the hardened surfaces was examined. All these were performed in order to replace the old worn bushing with the new designed one in Mercedes Unimog military vehicle. This study deals with the induction hardening and wear phenomena rather than the designation and production of the bushing.

2. EXPERIMENTAL METHOD

The chemical composition of 100Cr6 steel is given Table 1. These values were obtained by averaging four burnings at spectral analysis device.

Table 1. Chemical composition of 100Cr6 steel (%w)

| | | | |
|-----|-------|-----|-------|
| C: | 0,995 | S: | 0,002 |
| Mn: | 0,444 | Mo: | 0,028 |
| Si: | 0,223 | Al: | 0,019 |
| Cr: | 1,401 | Cu: | 0,172 |
| P: | 0,006 | Ni: | 0,085 |

Technical drawing of the designed bushing is given in Figure 1. For this purpose, cylindrical steel rods in 55 mm diameter were supplied. The rods were machined to 52,7 mm diameter and cut in 57 mm length. Then, induction hardening procedure was performed on the outer surfaces of these solid rods via Inductoscan-Sp device. Manufacturing of the bushing is not the main goal of this study. It is aimed to have enough hardened layer on the rod so that the outer surface of the bushing will remain within the induction hardened layer of the solid rod. The induction heating power was 100 kW, and the frequency was kept constant at 10 kHz. The samples rotated at a speed of 15 rpm as they passed through the coil at a translational speed of 3 mm/sec. These induction parameters were chosen according to the previous experiences to achieve the best surface hardness and hardness depth combination.

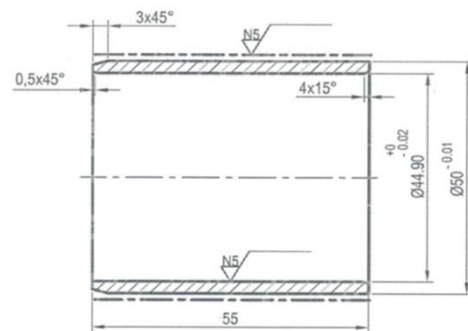


Figure 1. Technical drawing of the designed bushing

Rockwell C scale hardness of untreated steel was determined by using Mettest type device and averaging the five measurements. In order to

determine the induction hardened layer of the steel rod, Vickers hardness measurements were carried out under 30 kg load for 12 seconds and averaged five tests. Eight Vickers hardness tests at 0,5 mm intervals from outside through inside of hardened rod surfaces were applied.

The supplied and induction hardened steel samples were grinded and polished by standard metallographic techniques. After etching the polished surfaces with 5% nital solution, microstructures were obtained by Nikon metal microscope.

Wear tests were performed at room temperature in dry sliding conditions via a ball-on disc wear tester on the hardened surfaces of the rods. Wear tests were carried out at 4,92 mm/s sliding speed and under various loads (2,5/5/10 N). The abrasive ball is tungsten carbide (nearly 94%), the diameter and hardness values of the ball are 5 mm and 1500 HV₁, respectively. At least three wear tests were applied for each loading conditions. The samples were cleaned by alcohol and dried before and after each wear tests. The mass losses were calculated by measuring samples before and after wear tests using a balance with an accuracy of 10⁻⁴ g. The coefficients of friction were also recorded by the testing machine during the wear tests.

3. RESULTS AND DISCUSSION

The microstructures of untreated and induction hardened 100Cr6 steel were given in Figure 2. As seen in Figure 2a, the matrix structure of steel is pearlitic with carbides. A certain depth of martensitic structure with some retained austenite (white areas) is observed on induction hardened steel microstructure (Figure 2b). Due to high carbon content (0,995C %) of 100Cr6, martensite starting and finishing temperatures become lower. This leads to form an amount of retained (untransformed) austenite in martensitic structures. Under this layer, due to the absence of phase transformation the matrix is pearlitic again as expected (Figure 2c).

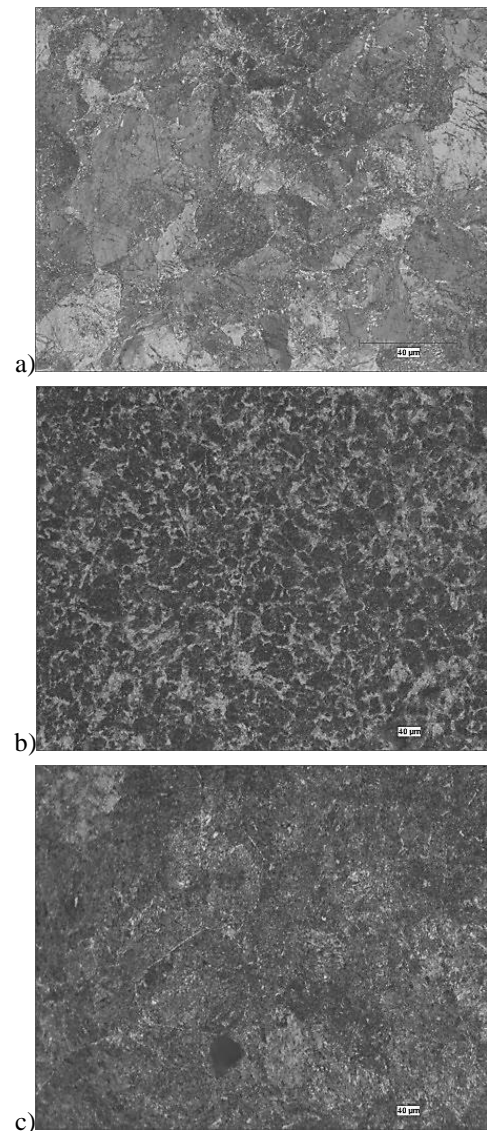


Figure 2. The microstructures of a) untreated steel, b) outside and c) inside of induction hardened steel

Rockwell hardness (with conversions in Brinell and Vickers values) and ultimate tensile strength values of the steel are given in Table 2. The hardness distribution from outside to inside of induction hardened steel rod is given in Figure 3. Approximately, 3 mm hardened layer was obtained by the applied induction hardening process parameters. This layer thickness provides the required dimensions of the designed bushing (Figure 1). In other words, after finishing process of manufacturing, there will be still enough hardened layer on the surface of the bushing.

Table 2. The hardness and ultimate tensile strength values

| Hardness | | | Ultimate tensile strength [MPa] |
|----------|-----|-----|---------------------------------|
| HRc | HB | HV | |
| 33 | 311 | 327 | 1051 |

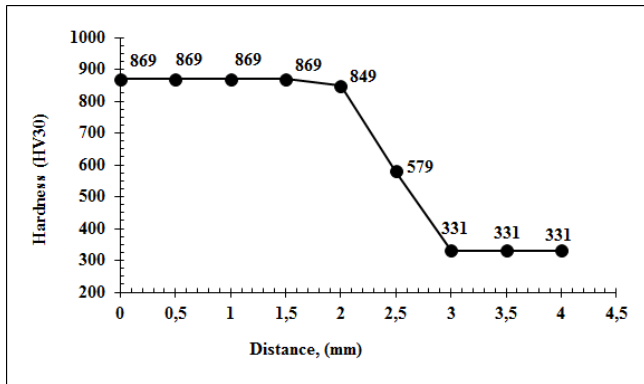


Figure 3. The hardness distribution from outside to inside

The mass losses of hardened steel relating with the applied normal loads (2.5, 5 and 10 N) are given in Figure 4. It is seen that less mass losses are obtained under small loads. Contrary to this, wear amount under 10 N load is observed less than the one obtained under 5 N load. When the load is increased from 2.5 N to 5 N, the mass loss is also increased nearly five times. But increasing the load from 5N to 10N did not provide an expected increase. As it is well known, higher normal loads will induce more frictional heat on working surfaces. When this is combined with the mechanical effect, plastic deformation takes place on surface, inducing work hardening by increased dislocation density and transforming retained austenite to martensite. This harder untempered martensitic phase formed during the wear tests may be the reason of less mass loss by higher load. Sipos et al. [10] reported that unlubricated hard steel surfaces of pearlitic structures can even transform into martensite by friction due to high surface temperatures and stresses. They called this brittle surface untempered martensite layer as a white layer.

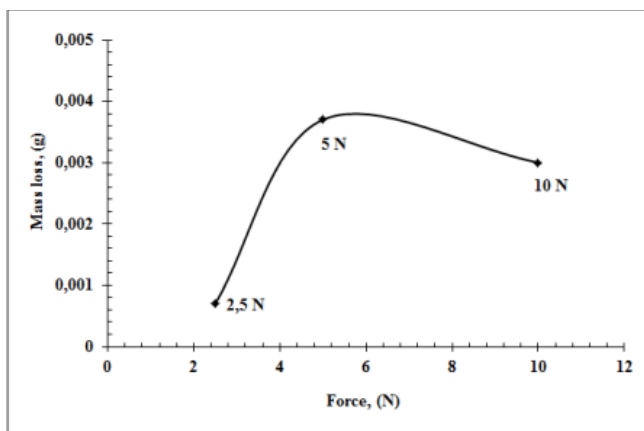


Figure 4. Mass losses under 2.5, 5 and 10 N loads

Surface roughness values (R_a and R_z) of steel samples before and after wear tests were given in

Table 3. It is seen that there is no noticeable variation in both R_a and R_z values after 2.5 N loading. However, these values increased 4-5 times more after 5N loading wear tests. Comparing the surface roughnesses of samples after 5 and 10 N loadings, it is seen that less enhancement in roughness values is obtained after 10N loading. Figure 4 verifies this result by illustrating more mass loss under 5 N load than that of 10 N.

Table 3. Surface roughness values in R_a and R_z before and after wear tests

| Surface roughness | | Before wear test | After loading of | | |
|-------------------|-------|------------------|------------------|------|------|
| | | | 2.5 N | 5 N | 10 N |
| Surface roughness | R_a | 0,05 | 0,06 | 0,28 | 0,37 |
| | R_z | 0,3 | 0,26 | 1,24 | 1,34 |

The variations of friction coefficients according to sliding distances were given in Figure 5 under the applied loads. The friction coefficients were changed in a wide range between 0.15-0.75 values when 2.5 N load was applied (Figure 5a). The most stable friction coefficient was obtained under 5N loading. At this loading condition, the friction coefficient reached a stable value (approximately 0.4) after a significant increase at the beginning. The fluctuations were in a narrow range between 0.35-0.50 values in this steady statement at 5 N loading. At 10 N loading, the friction coefficients fluctuated in a wide range (between 0.35-0.85) as it was at 2.5 N loading.

Güneş et al [11] reported that wear rates and friction coefficients of deep cryogenic treated (DCT) AISI 52100 steel samples, containing martensite, carbides and low amounts of retained austenite (maximum 5.7%) in their microstructure, increased as the amount of normal load increased (from 10N to 20N). Friction coefficients obtained under 5N and 10N loads in our study is well-matching with the above study. If we studied the wear performance under heavier loads than 10N, the effect of normal load on friction coefficient might be more clear.

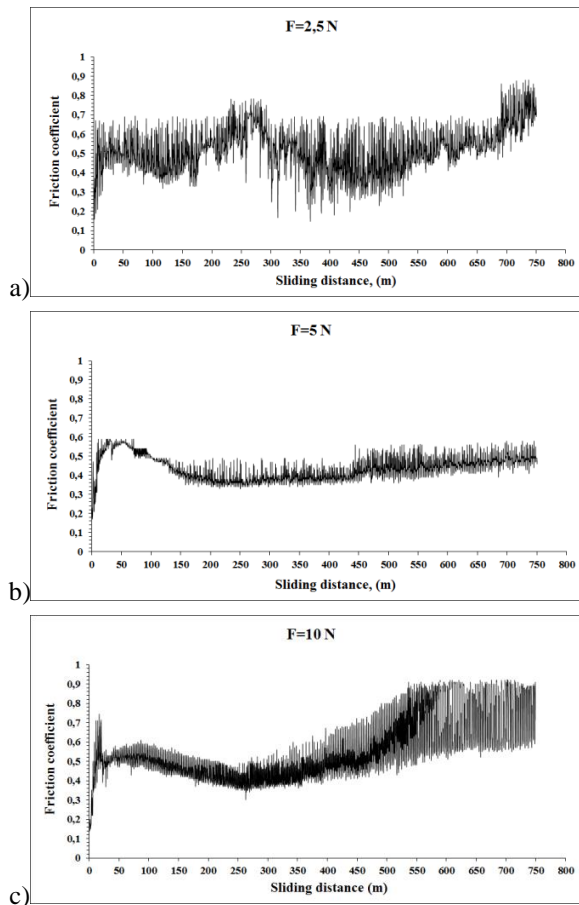


Figure 5. Friction coefficients at a)2.5 N, b)5 N and c)10 N loadings

The optic micrographs of wear tracks were illustrated at 200X magnification in Figure 6 for each loading conditions. The width of wear tracks were measured as 273, 360 and 209 μm under 2.5, 5 and 10N loads, respectively. The widest wear track was observed at 5 N loading in which an utmost mass loss was measured.

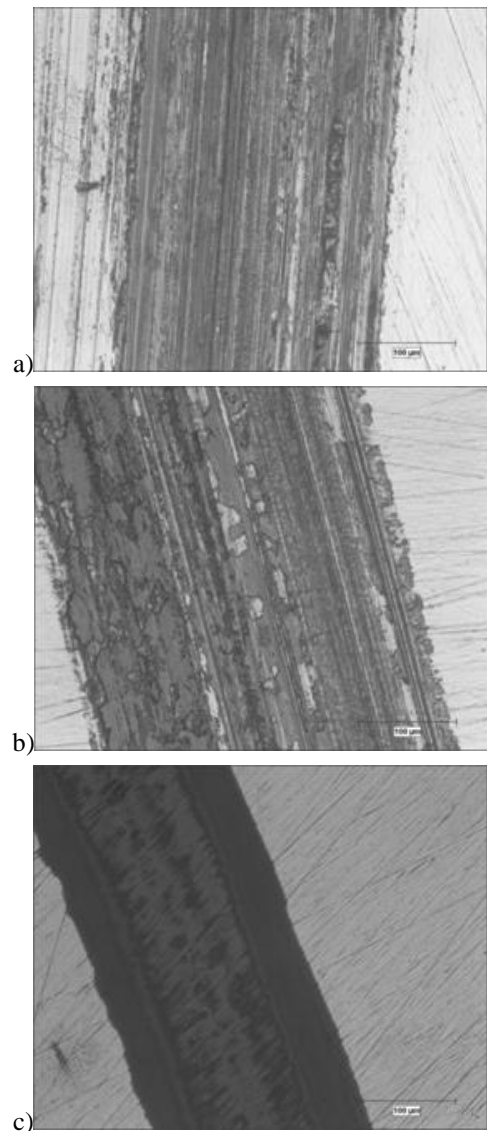


Figure 6. Wear tracks at a) 2.5 N, b) 5 N and c) 10 N loadings

SEM images of worn surfaces which is generated under 2.5, 5 and 10 N normal loads are shown in Figure 7. After loading of 2.5N as seen in Figure 7a, unclear surface grooves and some deformation marks are seen on the worn surface. The wear mechanism under this loading is not severe, possibly due to lower load than required. The predominant wear mechanism is adhesive at 5N and 10N normal loads(Figure 7b and c). This is more clearly seen at 5N loading. Smoother worn surface with less adhesive mechanism is seen after 10N loading due to the possible occurrence of hardening effect during sliding wear under this loading, as it was verified before by the low mass loss at this loading condition (Figure 4). Lin et al. [12] reported that the worn surface of ball bearing steel with a similar chemical composition to that of AISI 52000 became smoother with increasing surface hardness.

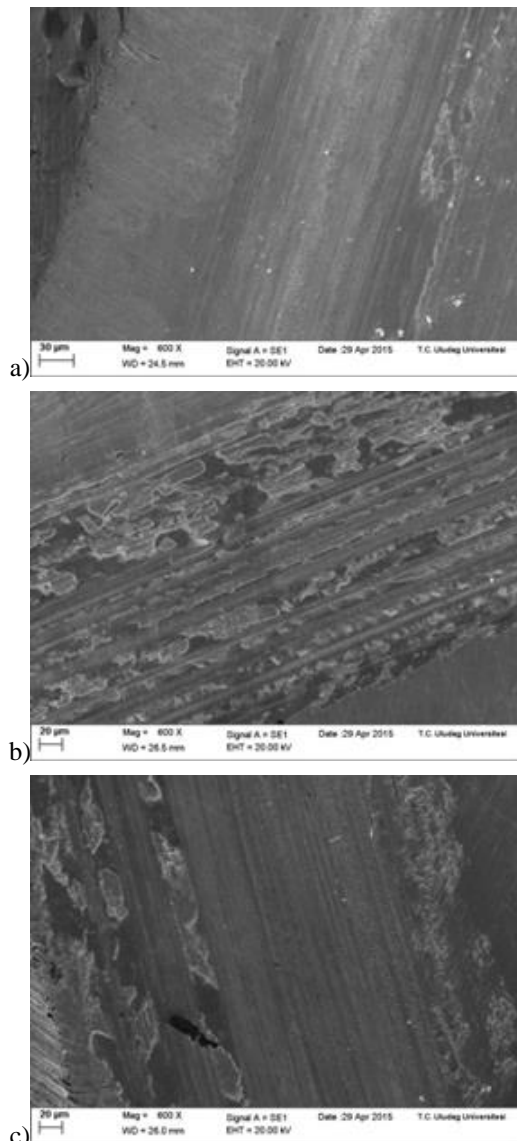


Figure 7. SEM graphs of worn surfaces at
a) 2.5 N, b) 5 N and c) 10 N loadings

4. CONCLUSIONS

The following results can be concluded in relation to induction hardening of 100Cr6 steel and then, ball-on disc type wearing under 2.5, 5 and 10 N loads.

- Nearly 3 mm depth of induction hardened layer was obtained by the applied process parameters.
- Martensite was formed at the outside of the steel and pearlite phase was remained inside.
- The utmost mass loss was obtained under 5 N loading as 0,0037 g, nearly five times more than that of 2.5 N loading. The least fluctuation, in other words, steady state in friction coefficients were also observed under 5 N loading condition.
- 2.5 N normal load did no effect on surface roughness value and provided a little mass

loss. This loading was quite low for making any significant change in induction hardened 100Cr6 steel.

- The designed bushing can be manufactured confidentially from the solid 100Cr6 steel rods of given dimensions by the applied induction hardening parameters.

ACKNOWLEDGEMENT

The authors would like to acknowledge and thank to the support of Turkish Land Forces 6th Maintenance Central Commandership.

REFERENCES

- [1] M. C. M. J. Schneider, "Introduction to surface hardening of steel," in *ASM Handbook, Heat Treating*, ASM International, vol. 4A, J. Dossett, Ed. 1991, pp. 259-267.
- [2] E. C. Santos, K. Kida, T. Honda, H. Koike A. J. Rozwadowska, "Fatigue strength improvement of AISI 52100 bearing steel by induction and repeated quenching," *Mater. Sci.*, vol.47, no.5, pp. 677-682, Mar 2012.
- [3] J. Grum, Induction heat treating, *Encyclopedia of tribology*, Springer, pp.1796-1808, 2013.
- [4] P. V. Krishna, R. R. Srikant, M. Iqbal, N. Sriram, "Effect of austempering and martempering on the properties of AISI 52100 steel," *ISRN Tribology*, vol. 2013, Article ID 515484, 6 pages, 2013.
- [5] V. Rudnev, G. A. Fett A. Griebel, J. Tartaglia, Principles of induction hardening and inspection, *ASM Handbook*, vol.4c, ASM International, 2014.
- [6] J. Yi, M. Gharghouri, P. Bocher, M. Medraj, "Distorsion and residual stress measurements of induction hardened AISI discs," *Mater. Chem. Phys.*, vol. 142, no. 1, pp. 248-258, oct 2013.
- [7] G. V. B. Lemos, T. K. Hirsch, A. S. Rocha, R. M. Nunes, "Residual stress analysis of drive shafts after induction hardening," *Mater. Res.*, vol. 17, no.1, pp. 70-74, Apr 2014.

- [8] M. Sharma, J. S. Kohli, S. Akhai, "Metallurgical analysis of cracks encountered during induction hardening of crankshafts," *Int. J. Res. Adv. Tech.*, vol.2,no. 4, pp. 295-304, Apr 2014.
- [9] A. Kusmoko, D. Dunne, R. Dahar, H. Li, "Surface treatment evaluation of induction hardened and tempered 1045 steel," *Int. j. curr.eng. tech.*, vol.4, no.3 pp. 1236-1239, june 2014.
- [10] K. Sipos, M. Lopez, M. Trucco, "Surface martensite white layer produced by adhesive sliding wear-friction in AISI 1065 steel," *Revista Latinoamerica de Metalurgia Materiales*, vol.28, no.1, pp. 46-50, june 2008.
- [11] İ. Güneş, A. Çiçek, K. Aslantaş, F. Kara, "Effect of deep cryogenic treatment on wear resistance of AISI 52100 bearing steel," *Trans Indian Inst Met*, vol. 67, no.6, pp. 909-917, may 2014.
- [12] P. Lin, Y. Zhu, H. Zhou, C. Wang, L. Ren, "Wear resistance of a bearing steel processed by laser surface remelting cooled by water, " *Scripta Mater.*, vol. 63, pp. 839-842, june 2010.